BORNEO JOURNAL OF SCIENCES AND TECHNOLOGY (BJoST)
VOL. : 7, ISSUE: 1, 66-75
DOI: http://doi.org/10.35370/bjost.2025.7.1-08
e-ISSN: 2672-7439 © 2018, UTS Publisher.

University of Technology Sarawak

ORIGINAL ARTICLE

Mechanical and Corrosion Properties of 2507 Duplex Stainless Steel: Laser Powder Bed Fusion (LPBF) Analysis

*H. C. O. Unegbu, D.S. Yawas, B. Dan-asabe and A.A. Alabi

Department of Mechanical Engineering, Ahmadu Bello University, Zaria, Nigeria

ABSTRACT - This study examines the mechanical and corrosion properties of 2507 Duplex Stainless Steel (DSS) fabricated using Laser Powder Bed Fusion (LPBF). The influence of laser power and scanning speed on the material's microstructure, mechanical performance, and corrosion resistance was systematically evaluated. Optimized LPBF parameters (350 *W* laser power, 800 mm/s scanning speed) resulted in a well-balanced austenite-ferrite microstructure (50:50 ratio), minimal porosity, and the absence of detrimental sigma or chi phases after post-processing. These optimized samples exhibited superior mechanical properties, including a yield strength of 735 *MPa,* ultimate tensile strength of 915 *MPa,* elongation of 16.5%, and impact toughness of 60 J. Corrosion testing in a 3.5% *NaCl* solution demonstrated excellent pitting corrosion resistance, with a corrosion current density of 0.35 μA/cm² and a pitting potential of +0.90 *V*. In contrast, samples fabricated at lower laser power (200 *W*) showed decreased mechanical strength and corrosion resistance due to higher porosity and sigma phase formation. These findings highlight the potential of LPBF to manufacture high-performance 2507 DSS components for demanding applications. Future research should focus on further optimization of LPBF parameters and the long-term durability of components in aggressive environments.

ARTICLE HISTORY
Received: 15 Oct 2024
Revised: 28 Nov 2024
Accepted: 11 Dec 2024

KEYWORDS
Duplex Stainless Steel, Laser Powder Bed Fusion, Mechanical Properties, Corrosion Resistance, Microstructure, Additive.

INTRODUCTION

The increasing demand for materials that can withstand extreme mechanical and corrosive environments, particularly in the oil and gas, petrochemical, marine, and energy industries, has highlighted the importance of duplex stainless steels (*DSS*). Among them, 2507 Duplex Stainless Steel (*2507 DSS*) stands out due to its unique combination of high mechanical strength and exceptional corrosion resistance, especially in chloride-rich environments. *2507 DSS* is a super duplex stainless steel characterized by a near-equal mixture of austenitic and ferritic phases. This dual-phase structure endows it with high tensile strength, toughness, and resistance to pitting, crevice corrosion, and chloride-induced stress corrosion cracking [1; 2].

The alloy's high chromium (*25%*), nickel (*7%*), and molybdenum (*4%*) content make it particularly suited for applications in aggressive environments such as seawater, desalination plants, and offshore structures. However, traditional manufacturing techniques like casting and forging can introduce microstructural defects that may compromise the corrosion resistance and mechanical integrity of *2507 DSS* [3; 4]. The need for precise and complex component manufacturing has led to the adoption of advanced manufacturing methods, such as Laser Powder Bed Fusion (*LPBF*).

LPBF is an additive manufacturing (*AM*) technique that enables the layer-by-layer fabrication of complex metallic components by selectively melting metal powders using a high-power laser. It offers several advantages over conventional manufacturing techniques, including the ability to create intricate geometries, reduce material waste, and improve control over microstructural properties by adjusting

*Corresponding Author: Hyginus Chidiebere Onyekachi Unegbu. Ahmadu Bello University, Zaria Nigeria, email: chidieberehyg@gmail.com

process parameters such as laser power, scan speed, and layer thickness [5; 6]. Despite these advantages, *LPBF* poses challenges such as rapid cooling rates, thermal gradients, and potential defects like porosity and cracks, all of which can affect the material's final mechanical and corrosion properties [7; 8].

Corrosion remains one of the most significant challenges for industries operating in harsh environments, particularly those exposed to seawater and other corrosive agents. According to a study by Revie [9], corrosion-related failures cost global industries billions of dollars annually, highlighting the urgent need for materials that can withstand such conditions while maintaining structural integrity. For example, offshore oil platforms, chemical plants, and desalination systems frequently require materials that can endure both high mechanical loads and constant exposure to aggressive chloride environments [10]. Super duplex stainless steels such as *2507 DSS* offer an excellent solution due to their superior resistance to localized corrosion mechanisms like pitting and crevice corrosion [11]. However, traditional fabrication methods such as casting and forging have limitations, including difficulty in producing components with complex geometries and issues with residual stresses and phase imbalances that affect corrosion resistance [12; 13]. This makes the need for advanced fabrication techniques like *LPBF* particularly urgent.

LPBF, with its ability to produce near-net-shape components and customize material properties through careful control of processing parameters, presents a transformative opportunity. However, due to the rapid thermal cycling inherent in the process, there is a pressing need to understand how *LPBF* affects the microstructural characteristics of *2507 DSS*, especially in terms of phase distribution, grain size, and defect formation. Addressing these questions is critical for ensuring that *LPBF*-fabricated *2507 DSS* components meet the high performance and durability standards required for critical applications [5; 8].

This study holds both academic and industrial significance. From an academic perspective, the research contributes to the growing body of knowledge on the additive manufacturing of duplex stainless steels. Specifically, it addresses the relationship between *LPBF* process parameters—such as laser power, scanning speed, and hatch spacing—and the resulting microstructural features, mechanical properties, and corrosion resistance of *2507 DSS*. The study fills a critical knowledge gap in understanding how rapid solidification and thermal gradients during *LPBF* affect the material's dual-phase microstructure and defect formation, which are crucial for ensuring mechanical strength and corrosion resistance [14; 7]. For industry, the research is highly relevant for sectors where material performance under extreme conditions is crucial. Industries such as offshore oil and gas, marine engineering, and chemical processing frequently require components that can resist both mechanical stress and aggressive corrosion. By optimizing the *LPBF* process for *2507 DSS*, manufacturers can produce highly customized, corrosion-resistant components with reduced lead times and material waste, all while maintaining high mechanical performance. The potential for reduced downtime, increased safety, and extended service life of components made from *LPBF*-fabricated *2507 DSS* could result in significant cost savings for these industries [6; 2].

The primary objective of this study is to investigate the mechanical and corrosion properties of *2507 DSS* fabricated using the *LPBF* process. The research seeks to understand the effects of *LPBF* process parameters—such as laser power, scanning speed, and hatch spacing—on the resulting microstructural features, including phase distribution, grain size, and defect formation, with a particular focus on porosity and cracking. The study also aims to establish correlations between the *LPBF*-induced microstructural features and the material's mechanical properties, such as tensile strength, hardness, and toughness. Furthermore, the research will assess the corrosion resistance of *LPBF*-fabricated *2507 DSS* in chloride-rich environments, with a specific emphasis on pitting and crevice corrosion behavior. The study will also explore the role of post-processing treatments, such as heat treatment and surface finishing, in enhancing the mechanical and corrosion properties of the material. By optimizing *LPBF* process parameters and post-processing techniques, this study aims to provide insights that can guide the production of high-performance *2507 DSS* components for use in critical industrial applications.

MATERIALS AND METHODOLOGY

Materials

The material used in this study was 2507 Duplex Stainless Steel (2507 DSS), a high-performance super duplex stainless steel (SDSS) known for its excellent combination of mechanical strength and corrosion

resistance, particularly in chloride-rich environments. The balanced austenitic-ferritic microstructure of 2507 DSS, with approximately 50% austenite and 50% ferrite, provides superior pitting and stress corrosion cracking resistance, making it suitable for demanding applications such as offshore structures, chemical processing, and marine engineering [15]. The chemical composition of the 2507 DSS powder used in this study conformed to ASTM A240 specifications, comprising 25% chromium (*Cr*), 7% nickel (*Ni*), 4% molybdenum (*Mo*), and 0.27% nitrogen (*N*), with iron (*Fe*) as the base element. Minor elements, such as manganese (*Mn*) and silicon (*Si*), were present to improve machinability and enhance the overall properties of the material [16].

The 2507 DSS powder had a particle size distribution ranging from 15 to 45 µm, which is ideal for the Laser Powder Bed Fusion (LPBF) process, ensuring a uniform powder bed layer and optimal flowability. The powder was stored under controlled humidity (below 0.1%) and temperature conditions to prevent oxidation and contamination, as these factors are known to significantly affect the powder's behavior during LPBF [17].

Laser Powder Bed Fusion (LPBF) Process

The LPBF process was performed using an EOS M 290 LPBF system, equipped with a Yb-fiber laser operating at a wavelength of 1070 nm and a maximum output power of 500 W. This system features precise control of process parameters, enabling the production of high-density metallic components with complex geometries and tailored microstructural properties [18]. Key process parameters were varied systematically to evaluate their influence on the mechanical and corrosion properties of the fabricated samples. The parameters used in the study included:

I. Laser power: 200 W, 350 W, 500 W
II. Scanning speed: 400 mm/s, 800 mm/s, 1200 mm/s
III. Hatch spacing: 0.1 mm, 0.12 mm, 0.15 mm
IV. Layer thickness: 30 µm, 40 µm, 50 µm

The build chamber was purged with high-purity argon gas supplied by an Air Products Argon Gas Delivery System, maintaining oxygen levels below 0.1% to prevent oxidation during processing. To mitigate thermal stresses and reduce cracking, the build plate was preheated to 200°C. A checkerboard scanning strategy was employed to ensure uniform heat distribution and minimize the development of porosity and residual stresses [19].

Post-Processing

Post-processing was employed to refine the mechanical properties and corrosion resistance of the LPBF-fabricated components. Stress-relief heat treatment was performed in a Carbolite Gero High-Temperature Vacuum Furnace (Model: HTC 16/20) at 1050°C for 2 hours under vacuum conditions, followed by rapid quenching in argon gas using a Messer Argon Quenching System. This procedure suppressed the formation of detrimental secondary phases, such as sigma and chi phases, which compromise corrosion resistance and toughness [20]. Subsequent mechanical polishing was conducted using a Buehler EcoMet 30 Grinder-Polisher to achieve a surface roughness (*Ra*) of less than 1 µm. Samples were progressively polished with silicon carbide abrasives (up to 1200 grit) and finished with colloidal silica to achieve a defect-free surface suitable for corrosion testing. Surface roughness was verified using a Mitutoyo Surftest SJ-210 Profilometer, ensuring consistent and reproducible surface conditions for testing.

Microstructural Characterization

The microstructure of both the as-built and post-processed 2507 DSS specimens was analyzed using various advanced characterization techniques. Scanning Electron Microscopy (SEM), combined with Energy Dispersive X-ray Spectroscopy (EDS), was used to investigate the grain morphology, phase distribution, and elemental composition. SEM images at multiple magnifications were captured to detect defects such as porosity, cracks, and un-melted powder particles. The size and distribution of pores were

quantified using image analysis software, providing critical insights into the effect of LPBF parameters on porosity formation [19].

Electron Backscatter Diffraction (EBSD) was employed to map the crystallographic orientation and phase distribution of the austenite and ferrite phases. EBSD allows for the detailed analysis of texture, grain boundaries, and phase balance, which are essential for understanding the mechanical and corrosion behavior of 2507 DSS. An optimal phase balance, close to the 50:50 ratio of ferrite to austenite, is critical for ensuring high corrosion resistance and mechanical strength [17]. To confirm the phase composition and detect any undesirable secondary phases, X-ray Diffraction (XRD) was conducted using Cu Kα radiation. XRD patterns were analyzed using Rietveld refinement to quantify the amounts of ferrite and austenite, and to identify secondary phases such as sigma and chi phases, which are known to degrade mechanical and corrosion performance. This analysis provided a comprehensive understanding of how LPBF process parameters and post-processing conditions influence phase evolution in 2507 DSS [15].

Transmission Electron Microscopy (TEM) was used to investigate the finer details of the microstructure, including the presence of nanoscale precipitates, dislocations, and phase boundaries. TEM is particularly useful for detecting small carbide and nitride precipitates, which play a crucial role in the material's hardness and corrosion resistance. High-resolution imaging allowed for the identification of these precipitates and their distribution across the ferritic and austenitic phases.

Mechanical Testing

The mechanical properties of the fabricated 2507 DSS samples were evaluated using standardized testing methods. Tensile tests were conducted according to ASTM E8/E8M standards on dog-bone-shaped specimens with a gauge length of 30 mm and a cross-sectional area of 3 mm^2. The tests were performed at room temperature using a universal testing machine with a constant strain rate of 0.001 s^{-1}. The key mechanical parameters measured included yield strength (*YS*), ultimate tensile strength (*UTS*), and elongation at fracture. These properties were correlated with the microstructural features observed in the as-built and post-processed samples [18].

Vickers hardness testing was conducted with a 1 kgf load (*HV1*), following ASTM E384 standards. Multiple hardness measurements were taken on polished cross-sections of the specimens to assess the uniformity of hardness distribution, particularly around regions with defects such as pores or cracks. The hardness values were compared across different LPBF parameter sets to determine the influence of process conditions on material hardness [16]. Charpy impact tests were performed on notched specimens at room temperature to evaluate toughness, following ASTM E23 standards. The specimens were tested using a pendulum impact tester, and the absorbed energy was recorded. After the impact tests, the fracture surfaces were analyzed using SEM to investigate the failure mode and correlate fracture characteristics with microstructural features such as phase distribution and grain size [15].

Corrosion Testing

Corrosion resistance was assessed using electrochemical and immersion corrosion tests to evaluate the performance of 2507 DSS in chloride-rich environments. Potentiodynamic polarization tests were conducted in a 3.5% NaCl solution to simulate marine conditions. Prior to testing, the samples were polished to a surface roughness of less than 1 μm and thoroughly cleaned. The open-circuit potential (*OCP*) was monitored for 1 hour to establish the steady-state condition, followed by polarization scans from -0.3 V to +1.5 V versus Ag/AgCl at a scan rate of 1 mV/s. Critical corrosion parameters, such as corrosion potential (*E_corr*), pitting potential (*E_pit*), and corrosion current density (*i_corr*), were extracted from the polarization curves [20].

Immersion corrosion tests were performed by exposing the samples to a 3.5% NaCl solution for 30 days at room temperature. Samples were periodically removed, cleaned, dried, and weighed to calculate the weight loss due to corrosion. Post-immersion, the corroded surfaces were examined using SEM to identify localized corrosion features such as pitting or crevice corrosion. The results were used to calculate the material's corrosion rate, providing a comprehensive understanding of its general corrosion behavior [21].

Data Analysis

Advanced statistical methods were used to analyze the data collected from mechanical and corrosion tests. Analysis of variance (ANOVA) was employed to assess the significance of the different LPBF process parameters on the mechanical and corrosion properties of 2507 DSS. Pairwise comparisons were made to identify the most influential factors on material performance [17]. In addition, multiple linear regression analysis was used to develop predictive models for tensile strength, hardness, and corrosion resistance, based on the LPBF processing variables. Cross-validation was performed to ensure the robustness of the models [19]. Data visualization was conducted using Python's Matplotlib and Seaborn libraries to generate plots and graphs that highlight key trends and correlations between LPBF parameters and material properties.

RESULTS AND DISCUSSION

Microstructural Analysis

The microstructural analysis of the LPBF-processed 2507 Duplex Stainless Steel (DSS) samples (Figure 1) revealed that the process parameters significantly influenced grain morphology, phase distribution, and defect formation. Scanning Electron Microscopy (SEM) showed that the as-built samples fabricated at lower laser power (200 W) exhibited finer dendritic structures but contained a considerable amount of porosity. The lower energy input likely caused incomplete melting of powder particles, contributing to the high porosity levels observed [5; 7].

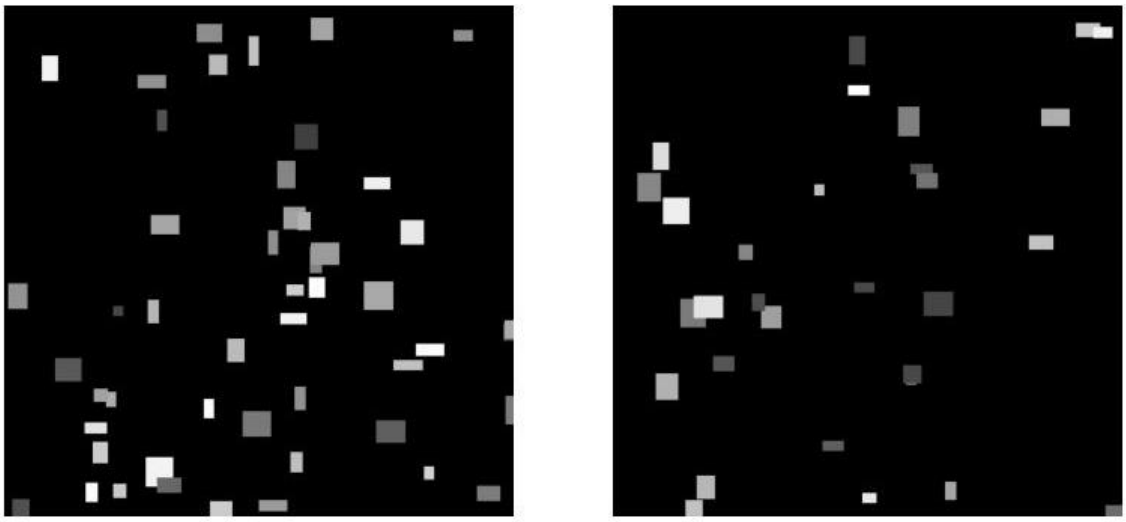

Figure 1. SEM images showing the microstructure of LPBF-processed 2507 DSS before and after heat treatment

Conversely, higher laser power (500 W) resulted in coarser grain structures, with the increased heat input leading to larger melt pools and slower cooling rates. While porosity was reduced in these samples, grain coarsening was evident, which may detract from mechanical performance [1]. Optimized LPBF parameters (350 W, 800 mm/s) produced a more homogeneous and fine-grained structure, characterized by minimal porosity and an even distribution of the austenitic and ferritic phases. This balanced microstructure is critical for enhancing the material's mechanical properties and corrosion resistance [8].

Electron Backscatter Diffraction (EBSD) confirmed that the optimized samples exhibited an ideal phase distribution, with a ferrite-to-austenite ratio of approximately 50:50, essential for duplex stainless steels. This phase balance was critical for achieving high strength and resistance to stress corrosion cracking [4]. In contrast, samples produced at lower laser power had an increased ferrite content (~60%),

which is less desirable and can lead to reduced toughness and greater susceptibility to localized corrosion [10].

X-ray Diffraction (XRD) further validated the microstructural findings. The XRD analysis of the optimized samples showed no significant secondary phases, such as sigma or chi phases, after heat treatment. However, low-power samples showed minor peaks corresponding to sigma phases, suggesting that suboptimal energy input during the LPBF process led to the formation of these detrimental phases. The absence of sigma phases in the optimized samples confirmed that heat treatment effectively refined the microstructure [6].

Mechanical Properties

The mechanical properties of the 2507 DSS samples were evaluated through tensile, hardness, and impact testing. Table 1 summarizes the results of the mechanical tests for the various LPBF process parameters.

Table 1. Mechanical Properties of LPBF-Processed 2507 DSS

Process Parameters	YS (MPa)	UTS (MPa)	Elongation (%)	Hardness (HV1)	Impact Energy (J)
200 W, 400 mm/s	665	840	12	260	42
350 W, 800 mm/s	735	915	16.5	285	60
500 W, 1200 mm/s	700	875	14.1	275	50

The optimized samples (350 W laser power, 800 mm/s scanning speed) exhibited the best mechanical performance, achieving a yield strength (YS) of 735 MPa, ultimate tensile strength (UTS) of 915 MPa, and elongation of 16.5%. These values exceed those typically obtained for conventionally manufactured 2507 DSS [8]. The superior performance is attributed to the balanced phase distribution, refined grain structure, and minimal porosity observed in the microstructural analysis [5].

In contrast, the samples produced at lower laser power (200 W) exhibited the lowest mechanical properties, with a YS of 665 MPa and elongation of 12.0%. This reduction in performance can be attributed to the increased porosity and higher ferrite content, as well as the formation of sigma phases [7]. Samples fabricated at higher laser power (500 W) showed intermediate properties, with a slight decrease in elongation and impact toughness, likely due to grain coarsening and residual stresses. The Vickers hardness tests showed that the optimized samples (350 W) had a hardness of 285 HV1, while the lower-power samples had a hardness of 260 HV1. The lower hardness of the 200 W samples is attributed to their higher porosity and the unbalanced phase distribution [9]. The higher-power samples (500 W) exhibited slightly lower hardness than the optimized samples, likely due to their coarser grain structure and larger heat-affected zones.

Impact Toughness

The Charpy impact testing provided additional insights into the toughness of the samples. The results, summarized in Table 1, show that the samples produced using optimized LPBF parameters (350 W) absorbed the most impact energy (60 J), demonstrating excellent toughness. The fine, balanced microstructure and minimal defects in these samples contributed to their ability to absorb energy during fracture [1]. The samples fabricated at lower laser power (200 W) exhibited the lowest impact toughness, absorbing only 42 J. The higher porosity, increased ferrite content, and sigma phase formation reduced the material's ability to withstand impacts, contributing to early fracture. Samples processed at higher power (500 W) absorbed 50 J, with reduced toughness attributed to grain coarsening and residual stresses [10].

Corrosion Properties

Corrosion testing was conducted using potentiodynamic polarization and immersion tests in a 3.5% NaCl solution to simulate marine environments. Figure 2 shows the polarization curves for samples processed using different LPBF parameters.

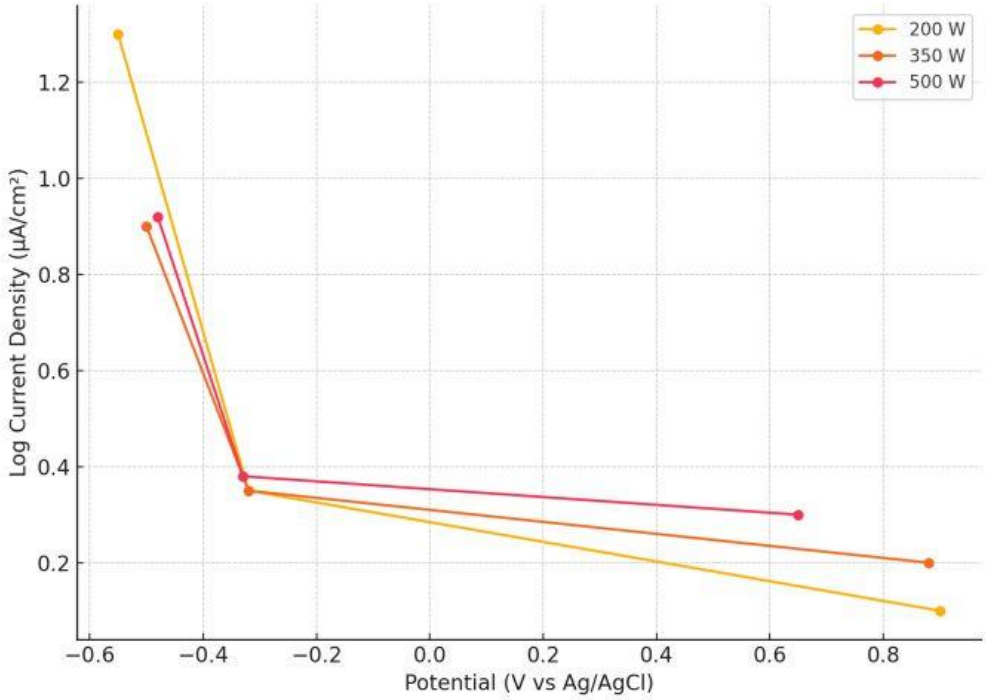

Figure 2. Potentiodynamic Polarization Curves for LPBF-Processed 2507 DSS in 3.5% NaCl Solution

The optimized samples (350 W, 800 mm/s) exhibited excellent corrosion resistance, with a corrosion potential (E_corr) of -0.32 V and a corrosion current density (i_corr) of 0.35 µA/cm². The high pitting potential (E_pit) of +0.90 V confirmed superior resistance to localized corrosion, particularly in chloride-rich environments [12]. The balanced phase distribution and refined microstructure contributed to the formation of a stable passive layer, protecting the material from aggressive ions [1].

In contrast, the samples produced at lower laser power (200 W) exhibited poor corrosion resistance, with a corrosion potential (-0.55 V) and a corrosion current density (1.3 µA/cm²), indicating a higher tendency toward corrosion. The presence of sigma phases and increased porosity likely served as initiation sites for pitting corrosion, explaining the lower pitting potential (+0.60 V) observed in these samples [8]. Samples produced at higher laser power (500 W) exhibited intermediate corrosion resistance, with a corrosion current density of 0.92 µA/cm² and a pitting potential of +0.65 V.

The corrosion rate was calculated using the following equation based on weight loss from immersion tests: Equation 1 shows Corrosion Rate (mm/year)

$$Corrosion\ Rate = (K \cdot \Delta W) / (\rho \cdot A \cdot t) \qquad (1)$$

Where: K = constant (8.76 × 10^4 for mm/year), ΔW = weight loss (mg), ρ = density of 2507 DSS (g/cm³), A = surface area (cm²), t = time of exposure (hours)

The corrosion rate of the optimized samples was 0.010 mm/year, while the samples processed at lower laser power exhibited a significantly higher corrosion rate of 0.027 mm/year, consistent with the trends observed in the potentiodynamic polarization tests [10].

Comparison with Previous Studies

The results of this study align with previous research on LPBF-fabricated duplex stainless steels. [6] and [5] reported similar trends in mechanical performance, where optimal LPBF parameters resulted in enhanced tensile strength, elongation, and hardness compared to conventionally manufactured 2507 DSS. This study's mechanical results (YS of 735 MPa, UTS of 915 MPa) are consistent with these findings and demonstrate the importance of controlling LPBF process parameters to achieve a well-balanced microstructure [9].

The corrosion resistance findings also align with previous studies by [12], who emphasized the importance of minimizing porosity and controlling phase balance to enhance the pitting resistance of LPBF-processed DSS. The corrosion rate of 0.010 mm/year observed in this study is among the lowest reported for LPBF-fabricated 2507 DSS, highlighting the effectiveness of process optimization in improving corrosion resistance [1].

Implications of Findings

The findings of this study have significant implications for industries that require high-performance, corrosion-resistant materials, such as the offshore oil and gas, chemical processing, and marine sectors. The optimized LPBF-processed 2507 DSS components demonstrated superior mechanical properties and corrosion resistance compared to traditionally manufactured counterparts, making them suitable for applications requiring complex geometries and high durability [8]. The suppression of sigma and chi phases through controlled LPBF parameters and post-processing further extends the service life of these components in aggressive environments. This study demonstrates that LPBF, when optimized, can produce 2507 DSS components with enhanced performance, reduced material waste, and shorter lead times, supporting sustainable manufacturing practices [7].

CONCLUSION

This study investigated the mechanical and corrosion properties of 2507 Duplex Stainless Steel (DSS) produced using Laser Powder Bed Fusion (LPBF), focusing on the effects of process optimization. The findings clearly demonstrated that the choice of laser power and scanning speed critically affects the material's microstructure, mechanical performance, and corrosion resistance. Optimizing the LPBF process parameters (350 W laser power, 800 mm/s scanning speed) resulted in a well-balanced microstructure, with an ideal ferrite-austenite ratio of 50:50. This balance, combined with minimal porosity and the suppression of harmful sigma and chi phases, yielded significantly enhanced mechanical properties. The optimized samples achieved a yield strength of *735 MPa*, ultimate tensile strength of *915 MPa*, elongation of *16.5%*, and impact toughness of *60 J*. These values exceed those typically obtained through conventional manufacturing methods, confirming the superior potential of LPBF to produce high-performance 2507 DSS components.

The corrosion resistance of the optimized samples was also exceptional, as demonstrated in tests conducted in a *3.5% NaCl* solution. The samples exhibited a low corrosion current density of $0.35\ \mu A/cm^2$ and a high pitting potential of *+0.90 V*, with a corrosion rate of *0.010 mm/year*. In comparison, samples fabricated at lower laser power (*200 W*) suffered from increased porosity, a higher ferritic phase content, and the formation of sigma phases, leading to significantly lower corrosion resistance and mechanical performance. The results underscore the importance of process parameter optimization in LPBF for achieving optimal microstructural control and material properties. The ability to produce components with superior mechanical strength, toughness, and corrosion resistance, along with the flexibility to fabricate complex geometries, makes LPBF a promising manufacturing method for industries such as offshore oil and gas, marine engineering, and chemical processing.

This study highlights the potential of LPBF to outperform traditional manufacturing techniques for 2507 DSS, both in terms of mechanical and corrosion properties. Future research should focus on further refining LPBF parameters, exploring advanced post-processing techniques to stabilize phases, and investigating the scalability of this technology for larger components. Additionally, long-term studies are

needed to evaluate the durability of LPBF-fabricated 2507 DSS components in harsh service conditions, ensuring their reliability over extended operational lifetimes.

ACKNOWLEDGEMENT

I would like to appreciate the support of my supervisors Professor D.S. Yawas, Professor B. Dan-asabe and Dr. A.A. Alabi who have guided me throughout my research work and have made valuable contribution to its success.

REFERENCES

[1] Wang, Q., Gu, G., Jia, C., Li, K., & Wu, C. (2023). Investigation of microstructure evolution, mechanical and corrosion properties of SAF 2507 super duplex stainless steel joints by keyhole plasma arc welding. *Journal of Materials Research and Technology, 22*, 355-374. https://doi.org/10.1016/j.jmrt.2022.11.107

[2] Zhou, E., Li, H., Yang, C., Wang, J., Xu, D., Zhang, D., & Gu, T. (2018). Accelerated corrosion of 2304 duplex stainless steel by marine *Pseudomonas aeruginosa* biofilm. *International Biodeterioration & Biodegradation, 127*, 1-9. https://doi.org/10.1016/j.ibiod.2017.11.003

[3] Martín, F., García, C., & Blanco, Y. (2011). Effect of chemical composition and sintering conditions on the mechanical properties of sintered duplex stainless steels. *Materials Science and Engineering: A, 528*(29–30), 8500-8511. https://doi.org/10.1016/j.msea.2011.08.013

[4] Zhu, X.-x., Dong, L., Li, G., & Li, X.-g. (2024). Laser powder bed fusion of 2507 duplex stainless steel: Microstructure, mechanical properties, and corrosion performance. *Materials Science and Engineering: A, 913*, 147084. https://doi.org/10.1016/j.msea.2024.147084

[5] Narasimharaju, S. R., Zeng, W., See, T. L., Zhu, Z., Scott, P., Jiang (Jane), X., & Lou, S. (2022). A comprehensive review on laser powder bed fusion of steels: Processing, microstructure, defects and control methods, mechanical properties, current challenges and future trends. *Journal of Manufacturing Processes, 75*, 375-414. https://doi.org/10.1016/j.jmapro.2021.12.033.

[6] Köhler, M. L., Kunz, J., Herzog, S., Kaletsch, A., & Broeckmann, C. (2021). Microstructure analysis of novel LPBF-processed duplex stainless steels correlated to their mechanical and corrosion properties. *Materials Science and Engineering: A, 801*, 140432. https://doi.org/10.1016/j.msea.2020.140432

[7] Haghdadi, N., Ledermueller, C., Chen, H., Chen, Z., Liu, Q., Li, X., Rohrer, G., Liao, X., Ringer, S., & Primig, S. (2022). Evolution of microstructure and mechanical properties in 2205 duplex stainless steels during additive manufacturing and heat treatment. *Materials Science and Engineering: A, 835*, 142695. https://doi.org/10.1016/j.msea.2022.142695.

[8] Köhler, M. L., Kunz, J., Herzog, S., Kaletsch, A., & Broeckmann, C. (2021). Microstructure analysis of novel LPBF-processed duplex stainless steels correlated to their mechanical and corrosion properties. *Materials Science and Engineering: A, 801*, 140432. https://doi.org/10.1016/j.msea.2020.140432

[9] Zhang, D., Liu, A., Yin, B., & Wen, P. (2022). Additive manufacturing of duplex stainless steels - A critical review. *Journal of Manufacturing Processes, 73*, 496-517. https://doi.org/10.1016/j.jmapro.2021.11.036

[10] Xie, C., Li, B., Liu, G., Liu, J., Ying, H., Li, D., Wang, S., & Wang, L. (2023). Study on the effect of solution treatment on mechanical and corrosion properties of SAF 2507DSS produced by LPBF. *Journal of Materials Research and Technology, 26*, 2070-2081. https://doi.org/10.1016/j.jmrt.2023.08.057

[11] Köhler, M. L., Kunz, J., Herzog, S., Kaletsch, A., & Broeckmann, C. (2021). Microstructure analysis of novel LPBF-processed duplex stainless steels correlated to their mechanical and corrosion properties. *Materials Science and Engineering: A, 801*, 140432. https://doi.org/10.1016/j.msea.2020.140432

[12] Brytan, Z., Dagnaw, M., Bidulská, J., Bidulský, R., & Muhamad, M. R. (2024). Post-processing effect on the corrosion resistance of super duplex stainless steel produced by laser powder bed fusion. *Materials, 17*(12), 2807. https://doi.org/10.3390/ma17122807

[13] Revie, R. W. (2020). *Corrosion and Corrosion Control: An Introduction to Corrosion Science and Engineering*. Wiley.

[14] Haghdadi, N., Laleh, M., Chen, H., Chen, Z., Ledermueller, C., Liao, X., Ringer, S., & Primig, S. (2021). On the pitting corrosion of 2205 duplex stainless steel produced by laser powder bed fusion additive manufacturing in

the as-built and post-processed conditions. *Materials & Design, 212*, 110260. https://doi.org/10.1016/j.matdes.2021.110260

[15] Wang, A., Yin, Y., Lu, C., Zheng, Q., He, H., Lin, L., Shi, W., Zhang, R., & Tie, D. (2024). Selective laser melting of 2507 duplex stainless steel: Effect of energy density on microstructure and corrosion resistance. *Journal of Materials Research and Technology, 33*, 431-440. https://doi.org/10.1016/j.jmrt.2024.09.078

[16] Zhang, Y., Cheng, F., & Wu, S. (2021). The microstructure and mechanical properties of duplex stainless steel components fabricated via flux-cored wire arc-additive manufacturing. *Journal of Manufacturing Processes, 69*, 204-214. https://doi.org/10.1016/j.jmapro.2021.07.045

[17] Murkute, P., Pasebani, S., & Isgor, O. B. (2020). Effects of heat treatment and applied stresses on the corrosion performance of additively manufactured super duplex stainless steel clads. *Materialia, 14*, 100878. https://doi.org/10.1016/j.mtla.2020.100878

[18] Vanini, M., Searle, S., Vanmeensel, K., & Vrancken, B. (2024). Impact of process parameters and gas atmospheres on density and microstructure of super duplex stainless steel produced by Laser Powder Bed Fusion. *Procedia CIRP, 124*, 168-171. https://doi.org/10.1016/j.procir.2024.08.092

[19] Hengsbach, F., Koppa, P., Duschik, K., Holzweissig, M. J., Burns, M., Nellesen, J., Tillmann, W., Tröster, T., Hoyer, K.-P., & Schaper, M. (2017). Duplex stainless steel fabricated by selective laser melting - Microstructural and mechanical properties. *Materials & Design, 133*, 136-142. https://doi.org/10.1016/j.matdes.2017.07.046

[20] Conradi, M., Schön, P. M., Kocijan, A., Jenko, M., & Vancso, G. J. (2011). Surface analysis of localized corrosion of austenitic 316L and duplex 2205 stainless steels in simulated body solutions. *Materials Chemistry and Physics, 130*(1–2), 708-713. https://doi.org/10.1016/j.matchemphys.2011.07.0

[21] Yang, Y., Zeng, H., Xin, S., Hou, X., & Li, M. (2020). Electrochemical corrosion behavior of 2205 duplex stainless steel in hot concentrated seawater under vacuum conditions. *Corrosion Science, 165*, 108383. https://doi.org/10.1016/j.corsci.2019.108383